$\bar{B}_s^0 \to K\pi, KK$ decays and effects of the next-to-leading order contributions

Jing-Jing Wang,[1] Dong-Ting Lin,[1] Wen Sun,[1] Zhong-Jian Ji,[1] Shan Cheng,[1] and Zhen-Jun Xiao[1,2,*]

[1]*Department of Physics, Institute of Theoretical Physics, Nanjing Normal University, Nanjing, Jiangsu 210023, People's Republic of China*

[2]*Jiangsu Key Laboratory for Numerical Simulation of Large Scale Complex Systems, Nanjing Normal University, Nanjing 210023, People's Republic of China*

By employing the perturbative QCD (pQCD) factorization approach, we calculate the branching ratios and charge parity (*CP*)-violating asymmetries of the four $\bar{B}_s^0 \to K\pi$ and KK decays, with the inclusion of all known next-to-leading order (NLO) contributions. We find numerically that (a) the NLO contribution can interfere with the leading order (LO) part constructively or destructively for different decay modes; (b) the NLO contribution leads to a 22% decrease for the central values of the LO pQCD prediction for $\mathrm{Br}(\bar{B}_s^0 \to K^+\pi^-)$, but $\sim 50\%$ enhancement to the other three considered $\bar{B}_s$ decays, the agreement between the central values of the pQCD predictions and the data are therefore improved effectively after the inclusion of the NLO contributions; (c) for both $\bar{B}_s^0 \to K^+\pi^-$ and $\bar{B}_s^0 \to K^+K^-$ decays, the NLO pQCD predictions for the direct and mixing induced *CP*-violating asymmetries agree well with the measured values in both the sign and the magnitude; and (d) the theoretical errors of the pQCD predictions for decay rates are about 35% of the cental values and larger than that of the relevant data.

I. INTRODUCTION

The B and B_s decays are very interesting phenomenologically for the precision test of the standard model (SM) and for the searches for the signal of the new physics beyond the SM. But the B_s decays are considerably less studied than the well-known $B_{u,d}$ decays due to the rapid oscillations of B_s mesons and the shortage of B_s events collected. Since the start of the LHC running, a lot of B_s^0 events have been collected by the LHCb collaboration, and some $B_s^0 \to PP$ decays are already observed [1,2], such as the first observation of the direct charge parity (*CP*) violation in B_s decays [1]:

$$\mathcal{A}_{CP}(B_s^0 \to K^-\pi^+) = (0.27 \pm 0.04(\text{stat}) \pm 0.01(\text{syst})),$$
$$(1)$$

and the first measurement of the time-dependent *CP* violation in $B_s^0 \to K^+K^-$ [2]:

$$C_{KK} = 0.14 \pm 0.11(\text{stat}) \pm 0.03(\text{syst}),$$
$$S_{KK} = 0.30 \pm 0.12(\text{stat}) \pm 0.04(\text{syst}). \quad (2)$$

During the past decade, in fact, many charmless two-body hadronic $B_s^0 \to M_2 M_3$ decays (here M_i denotes the light mesons such as π, K, ρ, etc.) have been studied by employing the perturbative QCD (pQCD) factorization approach at the leading order (LO) level [3–5] or the partial next-to-leading order (NLO) level [6]. In this paper

we calculate the branching ratios and *CP*-violating asymmetries of the $\bar{B}_s^0 \to K\pi$ and KK decays by employing the pQCD factorization approach, with the inclusion of all currently known NLO contributions. These decay modes have also been studied, for example, by using the generalized factorization in Ref. [7] or by using the QCD factorization (QCDF) approach in Refs. [8–10].

In the pQCD factorization approach, almost all NLO contributions to $B_{u,d} \to M_2 M_3$ decays have been calculated up to now. And it is straightforward to extend these calculations to the cases for the similar $B_s \to M_2 M_3$ decays. The NLO pQCD predictions for those considered decay modes proved that the NLO contributions can play an important role in understanding the very large $\mathrm{Br}(B \to K\eta')$ [11,12] or the so-called "$K\pi$-puzzle" [13]. Here, we focus on the studies for the possible effects of the NLO contributions from various sources, such as the QCD vertex corrections (VC), the quark loops (QL), and the chromomagnetic penguins [8,14]. The newly known NLO twist-2 contribution [15] and NLO twist-3 contribution to the relevant form factors [16] will also be taken into account here. This way one can improve the reliability of the pQCD factorization approach effectively.

This paper is organized as follows. In Sec. II, we give a brief review about the pQCD factorization approach and present the LO decay amplitudes for the studied decay modes. In Sec. III, the NLO contributions from different sources are evaluated analytically. We calculate and show the pQCD predictions for the averaged branching ratios and *CP*-violating asymmetries of $\bar{B}_s^0 \to K\pi$ and KK decays in Sec. IV. The summary and some discussions are included in the final section.

*xiaozhenjun@njnu.edu.cn

II. THEORETICAL FRAMEWORK AND LO DECAY AMPLITUDES

A. Outlines of the pQCD approach

We consider the B_s^0 meson at rest for simplicity. Using the light-cone coordinates, we define the B_s^0 meson with the momentum P_1, the emitted meson M_2 with the momentum P_2 moving along the direction of $n = (1, 0, \mathbf{0}_T)$, and the recoiled meson M_3 with the momentum P_3 in the direction of $v = (0, 1, \mathbf{0}_T)$. Here, we also use x_i to denote the momentum fraction of a light antiquark in each meson:

$$P_1 = \frac{m_{B_s}}{\sqrt{2}}(1, 1, \mathbf{0}_T), \qquad P_2 = \frac{m_{B_s}}{\sqrt{2}}(1 - r_3^2, r_2^2, \mathbf{0}_T),$$

$$P_3 = \frac{m_{B_s}}{\sqrt{2}}(r_3^2, 1 - r_2^2, \mathbf{0}_T), \tag{3}$$

$$k_1 = \frac{m_{B_s}}{\sqrt{2}}(x_1, 0, \mathbf{k}_{1T}), \qquad k_2 = \frac{m_{B_s}}{\sqrt{2}}(x_2(1 - r_3^2), x_2 r_2^2, \mathbf{k}_{2T}),$$

$$k_3 = \frac{m_{B_s}}{\sqrt{2}}(x_3 r_3^2, x_3(1 - r_2^2), \mathbf{k}_{3T}), \tag{4}$$

where $r_i = m_i/m_{B_s}$ with $m_i = m_\pi$ or m_K here. When the light pion and kaon are the final state mesons, $r_i^2 < 0.01$ and can be neglected safely. The integration over the small components k_1^-, k_2^-, and k_3^+ will lead conceptually to the decay amplitudes,

$$\mathcal{A}(B_s \to M_2 M_3) \sim \int dx_1 dx_2 dx_3 b_1 db_1 b_2 db_2 b_3 db_3$$
$$\cdot \text{Tr}[C(t)\Phi_{B_s}(x_1, b_1)\Phi_{M_2}(x_2, b_2)$$
$$\times \Phi_{M_3}(x_3, b_3)H(x_i, b_i, t)S_t(x_i)e^{-S(t)}], \tag{5}$$

where b_i is the conjugate space coordinate of k_{iT}. In the above equation, $C(t)$ is the Wilson coefficient evaluated at scale t. The functions Φ_{B_s}, Φ_{M_2}, and Φ_{M_3} are the wave functions of the initial B_s meson and the final state meson M_2 and M_3, respectively. The hard kernel $H(k_1, k_2, k_3, t)$ describes the four-quark operator and the spectator quark connected by a hard gluon whose q^2 is in the order of $\bar{\Lambda}m_{B_s}$. The jet function $S_t(x_i)$ in Eq. (5) is one of the two kinds of Sudakov form factors relevant for the B_s decays considered, which come from the threshold resummation over the large double logarithms ($\ln^2 x_i$) in the end-point region. The function $e^{-S(t)}$ is the second kind of the Sudakov form factors. The Sudakov form factors effectively suppress the soft dynamics at the end-point region [17,18].

For the studied $\bar{B}_s^0 \to K\pi, KK$ decays, the corresponding weak effective Hamiltonian can be written as [19]

$$\mathcal{H}_{\text{eff}} = \frac{G_F}{\sqrt{2}}\left\{ V_{ub}V_{uq}^*[C_1(\mu)O_1^u(\mu) + C_2(\mu)O_2^u(\mu)] \right.$$

$$\left. - V_{tb}V_{tq}^*\left[\sum_{i=3}^{10} C_i(\mu)O_i(\mu)\right]\right\} + \text{H.c.}, \tag{6}$$

where $q = d, s$, $G_F = 1.16639 \times 10^{-5}$ GeV^{-2} is the Fermi constant, and V_{ij} is the Cabbibo-Kobayashi-Maskawa (CKM) matrix element, $C_i(\mu)$ are the Wilson coefficients evaluated at the renormalization scale μ, and $O_i(\mu)$ are the four-fermion operators.

As usual, we treat the B meson as a very good heavy-light system, and adopt the distribution amplitude ϕ_{B_s} as in Ref. [5]:

$$\phi_{B_s}(x, b) = N_{B_s}x^2(1 - x)^2 \exp\left[-\frac{M_{B_s}^2 x^2}{2\omega_b^2} - \frac{1}{2}(\omega_b b)^2\right], \tag{7}$$

where the shape parameter ω_b is a free parameter and we take $\omega_b = 0.5 \pm 0.05$ GeV for the B_s meson based on studies of lattice QCD and the light-cone sum rule [18], and finally the normalization factor N_{B_s} depends on the values of ω_b and the decay constant f_{B_s} and is defined through the normalization relation $\int_0^1 dx\phi_{B_s}(x, 0) = f_{B_s}/(2\sqrt{6})$.

For the light pseudoscalar mesons π and K, their wave functions are the same in form and can be defined as [20]

$$\Phi(P, x, \zeta) \equiv \frac{1}{\sqrt{2N_C}}\gamma_5[P\phi^A(x) + m_0\phi^P(x)$$
$$+ \zeta m_0(\not{n}\not{v} - 1)\phi_P^T(x)], \tag{8}$$

where P and x are the momentum of the light meson and the momentum fraction of the quark (or antiquark) inside the meson, respectively. When the momentum fraction of the quark (antiquark) is set to be x, the parameter ζ should be chosen as $+1$ (-1). The distribution amplitudes (DAs) of the light meson $M = (\pi, K)$ are adopted from Ref. [20,21]:

$$\phi_M^A(x) = \frac{3f_M}{\sqrt{6}}x(1 - x)[1 + a_1^M C_1^{3/2}(t) + a_2^M C_2^{3/2}(t)], \tag{9}$$

$$\phi_M^P(x) = \frac{f_M}{2\sqrt{6}}\left[1 + \left(30\eta_3 - \frac{5}{2}\rho_M^2\right)C_2^{1/2}(t)\right], \tag{10}$$

$$\phi_M^T(x) = \frac{f_M(1 - 2x)}{2\sqrt{6}}\left[1 + 6\left(5\eta_3 - \frac{1}{2}\eta_3\omega_3 - \frac{7}{20}\rho_M^2\right.\right.$$
$$\left.\left. - \frac{3}{5}\rho_M^2 a_2^M\right)(1 - 10x + 10x^2)\right], \tag{11}$$

with the mass ratio $\rho_M = (m_\pi/m_0^\pi, m_K/m_0^K)$ for $M = (\pi, K)$, respectively [11,14]. The Gegenbauer moments a_i^M and other input parameters are the same as in Ref. [5]:

$$a_1^\pi = 0, \qquad a_2^\pi = 0.44_{-0.20}^{+0.10},$$
$$a_1^K = 0.17 \pm 0.05, \qquad a_2^K = 0.20 \pm 0.06,$$
$$\eta_3 = 0.015, \qquad \omega_3 = -3.0. \tag{12}$$

The Gegenbauer polynomials $C_n^\nu(t)$ in Eqs. (9)–(11) can be found easily in Refs. [5,12]. For more details about recent

progress on the wave functions of heavy and light mesons, one can see Ref. [22] and references therein.

B. Decay amplitudes at the leading order

The four $\bar{B}_s^0 \to (K^+\pi^-, K^0\pi^0, K^+K^-, \bar{K}^0K^0)$ decays have been studied previously in Ref. [5] by employing the pQCD factorization approach at the leading order. The decay amplitudes as presented in Ref. [5] are

confirmed by our independent calculations. In this paper, we focus on the calculations of the NLO contributions to these decays. At the leading order, the relevant Feynman diagrams that may contribute to the $\bar{B}_s^0 \to K\pi, KK$ decays are illustrated in Fig. 1. For the sake of completeness, however, we first show the relevant LO decay amplitudes in this section based on our own analytical calculations.

$$
\mathcal{A}(\bar{B}_s^0 \to K^+\pi^-) = V_{ub}V_{ud}^* \cdot [f_\pi F_{eK}a_1 + M_{eK}C_1] - V_{tb}V_{td}^* \cdot \left\{ f_\pi F_{eK}(a_4 + a_{10}) \right.
$$
$$
+ f_\pi F_{eK}^{P_2}(a_6 + a_8) + M_{eK}(C_3 + C_9) + f_{B_s}F_{aK}\left(a_4 - \frac{1}{2}a_{10}\right)
$$
$$
\left. + f_{B_s}F_{aK}^{P_2}\left(a_6 - \frac{1}{2}a_8\right) + M_{aK}\left(C_3 - \frac{1}{2}C_9\right) + M_{aK}^{P_1}\left(C_5 - \frac{1}{2}C_7\right) \right\}, \tag{13}
$$

$$
\sqrt{2}\mathcal{A}(\bar{B}_s^0 \to K^0\pi^0) = V_{ub}V_{ud}^* \cdot [f_\pi F_{eK}a_2 + M_{eK}C_2] - V_{tb}V_{td}^* \cdot \left\{ -f_{B_s}F_{aK}\left(a_4 - \frac{1}{2}a_{10}\right) \right.
$$
$$
- (f_\pi F_{eK}^{P_2} + f_{B_s}F_{aK}^{P_2})\left(a_6 - \frac{1}{2}a_8\right) + M_{eK}\left(-C_3 + \frac{3}{2}C_8 + \frac{1}{2}C_9 + \frac{3}{2}C_{10}\right)
$$
$$
\left. + f_\pi F_{eK}\left(-a_4 - \frac{3}{2}a_7 + \frac{3}{2}a_9 + \frac{1}{2}a_{10}\right) - M_{aK}\left(C_3 - \frac{1}{2}C_9\right) - M_{aK}^{P_1}\left(C_5 - \frac{1}{2}C_7\right) \right\}, \tag{14}
$$

$$
\mathcal{A}(\bar{B}_s^0 \to K^+K^-) = V_{ub}V_{us}^* \cdot [f_k F_{eK}a_1 + M_{eK}C_1 + M_{aK}C_2] - V_{tb}V_{ts}^* \cdot \left\{ f_k F_{eK}(a_4 + a_{10}) \right.
$$
$$
+ f_k F_{eK}^{P_2}(a_6 + a_8) + M_{eK}(C_3 + C_9) + M_{eK}^{P_1}(C_5 + C_7) + f_{B_s}F_{aK}^{P_2}\left(a_6 - \frac{1}{2}a_8\right)
$$
$$
+ M_{aK}\left(C_3 + C_4 - \frac{1}{2}C_9 - \frac{1}{2}C_{10}\right) + M_{aK}^{P_1}\left(C_5 - \frac{1}{2}C_7\right)
$$
$$
\left. M_{aK}^{P_2}\left(C_6 - \frac{1}{2}C_8\right) + [M_{aK}(C_4 + C_{10}) + M_{aK}^{P_2}(C_6 + C_8)]_{K^+\leftrightarrow K^-} \right\}, \tag{15}
$$

$$
\mathcal{A}(\bar{B}_s^0 \to \bar{K}^0K^0) = -V_{tb}V_{ts}^* \cdot \left\{ f_k F_{eK}\left(a_4 - \frac{1}{2}a_{10}\right) + (f_k F_{eK}^{P_2} + f_{B_s}F_{aK}^{P_2})\left(a_6 - \frac{1}{2}a_8\right) \right.
$$
$$
+ M_{eK}\left(C_3 - \frac{1}{2}C_9\right) + (M_{eK}^{P_1} + M_{aK}^{P_1})\left(C_5 - \frac{1}{2}C_7\right) + M_{aK}\left(C_3 + C_4 - \frac{1}{2}C_9 - \frac{1}{2}C_{10}\right)
$$
$$
\left. + M_{aK}\left(C_4 - \frac{1}{2}C_{10}\right)_{K^0\leftrightarrow\bar{K}^0} + \left[M_{aK}^{P_2}\left(C_6 - \frac{1}{2}C_8\right) + [K^0\leftrightarrow\bar{K}^0]\right] \right\}, \tag{16}
$$

where a_i is the combination of the Wilson coefficients C_i, the same as in Ref. [5]. The nine individual decay amplitudes, such as F_{eK} and F_{eK}^{P2} that appeared in Eqs. (13)–(16), are obtained by evaluating the corresponding Feynman diagrams in Fig. 1 analytically. One can find the expressions for all these decay amplitudes easily in Ref. [5].

III. NEXT-TO-LEADING ORDER CONTRIBUTIONS

A. NLO contributions from different sources

For the considered decay modes, one should, first, use the NLO Wilson coefficients $C_i(M_W)$, the NLO RG evolution matrix $U(t, m, \alpha)$ [19], and the $\alpha_s(t)$ at the two-loop level in numerical calculations. Second, one should take all the
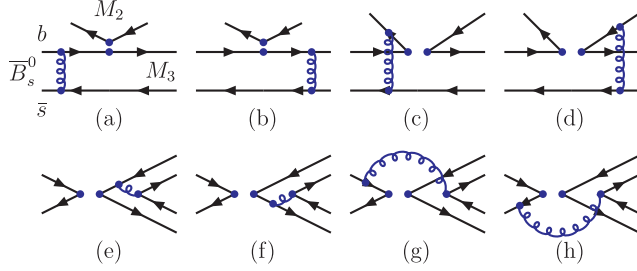
FIG. 1 (color online). Typical Feynman diagrams that may contribute at the leading order to $\bar{B}_s^0 \to K\pi, KK$ decays.

Feynman diagrams that lead to the decay amplitudes to be proportional to $\alpha_s^2(t)$ in the analytical evaluations. Such Feynman diagrams can be grouped into the following classes:

(1) The vertex corrections, as illustrated in Figs. 2(a)–2(d), the same set as in the QCDF approach.

(2) The NLO contributions from quark loops [14] and the chromomagnetic penguin operator O_{8g} [23], as illustrated in Figs. 2(e)–2(h).

(3) The NLO twist-2 and twist-3 contributions to the form factors of $B \to P$ ($P = \pi, K$, the light pseudoscalars) transitions [15,16], coming from the Feynman diagrams in Fig. 3.

(4) The NLO corrections to the LO hard spectator diagrams and annihilation diagrams, as illustrated in Fig. 5 of Ref. [12].

At present, only the calculations for the NLO corrections to the LO hard spectator and annihilation diagrams have not been completed yet. But from the comparative studies of the LO and NLO contributions from different sources in Refs. [12,13], we believe that those still unknown NLO contributions in the framework of the pQCD factorization approach, as the high order corrections to small LO contributions, are most possibly very small in size and could be neglected safely.
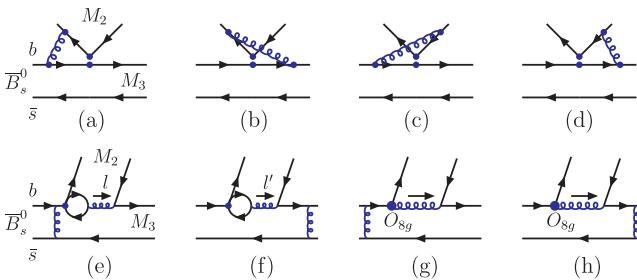

FIG. 2 (color online). Feynman diagrams for NLO contributions: the vertex corrections (a)–(d); the quark-loop contributions (e)–(f); and the chromomagnetic penguin contributions (g)–(h).
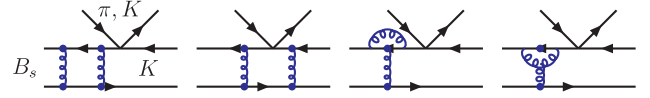

FIG. 3 (color online). The four typical Feynman diagrams, which contribute to the form factors of $B \to M_3$ transitions at the NLO level.

The vertex corrections to the factorizable emission diagrams, as illustrated by Figs. 2(a)–2(d), were calculated years ago in the QCD factorization approach [8,24]. For $B_s^0 \to K\pi, KK$ decays, the vertex corrections can be calculated without considering the transverse momentum effects of the quark at the end point [14], one can use the vertex corrections as given in Ref. [8] directly. The vertex corrections can then be absorbed into the redefinition of the Wilson coefficients $a_i(\mu)$ by adding a vertex function $V_i(M)$ to them. The expressions of the vertex functions $V_i(M)$ can be found easily in Refs. [8,14].

The contribution from the so-called quark loops is a kind of penguin correction with the four quark operators insertion, as illustrated by Figs. 2(e) and 2(f). For the $b \to s$ transition, the effective Hamiltonian $H_{\rm eff}^{ql}$, which describes the contributions from the quark loops, can be written as [14]

$$H_{\rm eff}^{(QL)} = -\sum_{q=u,c,t} \sum_{q'} \frac{G_F}{\sqrt{2}} V_{qb} V_{qs}^* \frac{\alpha_s(\mu)}{2\pi}$$
$$\times C^{(q)}(\mu, l^2)(\bar{s}\gamma_\rho(1-\gamma_5)T^a b)(\bar{q}'\gamma^\rho T^a q'), \quad (17)$$

where l^2 is the invariant mass of the gluon, as illustrated by Fig. 2(e). The expressions of the functions $C^{(q)}(\mu, l^2)$ for the loop of the $q(q = u, d, s, c, t)$ quark can be found, for example, in Ref. [14].

The magnetic penguin is another kind of penguin correction induced by the insertion of the operator O_{8g}, as illustrated by Figs. 2(g) and 2(h). The corresponding weak effective Hamiltonian containing the $b \to sg$ transition can be written as

$$H_{\rm eff}^{MP} = -\frac{G_F}{\sqrt{2}} V_{tb} V_{ts}^* C_{8g}^{\rm eff} O_{8g}, \quad (18)$$

where O_{8g} is the chromomagnetic penguin operator [19,23] and $C_{8g}^{\rm eff}$ is the corresponding effective Wilson coefficient: $C_{8g}^{\rm eff} = C_{8g} + C_5$ [14].

In Refs. [15,16], the authors calculated the NLO twist-2 and twist-3 contributions to the form factors $f^{+,0}(q^2)$ of the $B \to \pi$ transition. The NLO pQCD prediction for the form factor $f^+(q^2)$, for example, is of the form [16]

$$f^+(q^2)|_{\text{NLO}} = 8\pi m_B^2 C_F \int dx_1 dx_2 \int b_1 db_1 b_2 db_2 \phi_B(x_1, b_1)$$

$$\times \left\{ r_\pi [\phi_\pi^P(x_2) - \phi_\pi^T(x_2)] \cdot \alpha_s(t_1) \cdot e^{-S_{B\pi}(t_1)} \cdot S_t(x_2) \cdot h(x_1, x_2, b_1, b_2) \right.$$

$$+ [(1 + x_2\eta)(1 + F_{\text{T2}}^{(1)}(x_i, \mu, \mu_f, q^2))\phi_\pi^A(x_2) + 2r_\pi \left(\frac{1}{\eta} - x_2 \right) \phi_\pi^T(x_2) - 2x_2 r_\pi \phi_\pi^P(x_2)]$$

$$\cdot \alpha_s(t_1) \cdot e^{-S_{B\pi}(t_1)} \cdot S_t(x_2) \cdot h(x_1, x_2, b_1, b_2) + 2r_\pi \phi_\pi^P(x_2)(1 + F_{\text{T3}}^{(1)}(x_i, \mu, \mu_f, q^2))$$

$$\left. \cdot \alpha_s(t_2) \cdot e^{-S_{B\pi}(t_2)} \cdot S_t(x_2) \cdot h(x_2, x_1, b_2, b_1) \right\}, \tag{19}$$

where $\eta = 1 - q^2/m_B^2$ with $q^2 = (P_B - P_\pi)^2$, μ (μ_f) is the renormalization (factorization) scale, the hard scale $t_{1,2}$ is chosen as the largest scale of the propagators in the hard b-quark decay diagrams [15,16], the function $S_t(x_2)$ is the threshold resummation factor adopted from Ref. [25], the expressions of the hard function $h(x_i, b_j)$ can be found in Ref. [15,16], and, finally, the factor $F_{\text{T2}}^{(1)}(x_i, \mu, \mu_f, q^2)$ and $F_{\text{T3}}^{(1)}(x_i, \mu, \mu_f, q^2)$ describe the NLO twist-2 and twist-3 contribution to $f^{+,0}(q^2)$ of the $B \to \pi$ transition, respectively [15,16].

$$F_{\text{T2}}^{(1)}(x_i, \mu, \mu_f, q^2) = \frac{\alpha_s(\mu_f) C_F}{4\pi} \left[\frac{21}{4} \ln \frac{\mu^2}{m_B^2} - \left(\frac{13}{2} + \ln r_1 \right) \ln \frac{\mu_f^2}{m_B^2} + \frac{7}{16} \ln^2(x_1 x_2) + \frac{1}{8} \ln^2 x_1 \right.$$

$$+ \frac{1}{4} \ln x_1 \ln x_2 + \left(-\frac{1}{4} + 2 \ln r_1 + \frac{7}{8} \ln \eta \right) \ln x_1 + \left(-\frac{3}{2} + \frac{7}{8} \ln \eta \right) \ln x_2$$

$$\left. + \frac{15}{4} \ln \eta - \frac{7}{16} \ln^2 \eta + \frac{3}{2} \ln^2 r_1 - \ln r_1 + \frac{101\pi^2}{48} + \frac{219}{16} \right], \tag{20}$$

$$F_{\text{T3}}^{(1)}(x_i, \mu, \mu_f, q^2) = \frac{\alpha_s(\mu_f) C_F}{4\pi} \left[\frac{21}{4} \ln \frac{\mu^2}{m_B^2} - \frac{1}{2}(6 + \ln r_1) \ln \frac{\mu_f^2}{m_B^2} + \frac{7}{16} \ln^2 x_1 - \frac{3}{8} \ln^2 x_2 \right.$$

$$+ \frac{9}{8} \ln x_1 \ln x_2 + \left(-\frac{29}{8} + \ln r_1 + \frac{15}{8} \ln \eta \right) \ln x_1 + \left(-\frac{25}{16} + \ln r_2 + \frac{9}{8} \ln \eta \right) \ln x_2$$

$$\left. + \frac{1}{2} \ln r_1 - \frac{1}{4} \ln^2 r_1 + \ln r_2 - \frac{9}{8} \ln \eta - \frac{1}{8} \ln^2 \eta + \frac{37\pi^2}{32} + \frac{91}{32} \right], \tag{21}$$

where $r_i = m_B^2/\xi_i^2$ with the choice of $\xi_1 = 25m_B$ and $\xi_2 = m_B$ [15]. According to the analytical and numerical evaluations in Ref. [16], we get to know that the NLO twist-2 and NLO twist-3 contribution to the form factor of the $B \to \pi$ transition are similar in size but have an opposite sign, which leads to a strong cancellation between them and consequently results in a small total NLO contribution, $\sim 7\%$ variation to the full LO pQCD prediction for the case of $f^+(q^2)$ in the range of $0 \leq q^2 \leq 12$ GeV^2, as illustrated explicitly in Fig. 8 of Ref. [16].

In this paper we adopt the above NLO factors $F_{\text{T2}}^{(1)}(x_i, \mu, \mu_f, q^2)$ and $F_{\text{T3}}^{(1)}(x_i, \mu, \mu_f, q^2)$ directly, and then extend the expressions of $F_{\text{T2}}^{(1)}$ and $F_{\text{T3}}^{(1)}$ for the case of $B \to \pi$ to the case for $\bar{B}_s^0 \to K$ transition under the assumption of $SU(3)$ flavor symmetry, by making the proper replacements, such as $r_\pi = m_\pi/m_B \to r_k = m_k/m_{B_s}$, $m_B \to m_{B_s}$ and $\phi_\pi^{A,P,T} \to \phi_K^{A,P,T}$, for the expressions as given in Eqs. (20) and (21).

B. NLO decay amplitudes

For the sake of comparison and convenience, we denote all currently known NLO contributions except for those NLO twist-2 and twist-3 contributions to the form factors by the label "Set A," as described in the previous subsection. For the four considered $\bar{B}_s^0 \to K\pi, KK$ decays, the Set-A NLO contributions will be included in a simple way:

$$\mathcal{A}_{K\pi} \to \mathcal{A}_{K\pi} + \sum_{q=u,c,t} V_{qb}V_{qd}^* \mathcal{M}_{K^+\pi^-}^{(QL)} + V_{tb}V_{td}^* \mathcal{M}_{K^+\pi^-}^{(MP)}, \tag{22}$$

$$\mathcal{A}_{KK} \to \mathcal{A}_{KK} + \sum_{q=u,c,t} V_{qb}V_{qs}^* \mathcal{M}_{K^+K^-}^{(QL)} + V_{tb}V_{ts}^* \mathcal{M}_{K^+K^-}^{(MP)}, \tag{23}$$

where the quark-loop and magnetic penguin amplitudes $\mathcal{M}_{XY}^{(QL)}$ and $\mathcal{M}_{XY}^{(MP)}$ are of the form

$$
\begin{aligned}
\mathcal{M}_{K^+\pi^-}^{(QL)} = &-8m_{B_s}^4 \frac{C_F^2}{\sqrt{6}} \int_0^1 dx_1 dx_2 dx_3 \int_0^\infty b_1 db_1 b_3 db_3 \phi_{B_s}(x_1) \\
&\times \{[(1+x_3)\phi_\pi^A(x_2)\phi_K^A(x_3) + r_K(1-2x_3)\phi_\pi^A(x_2)(\phi_K^P(x_3)+\phi_K^T(x_3)) \\
&+ 2r_\pi\phi_\pi^P(x_2)\phi_K^A(x_3)] \cdot \alpha_s^2(t_a) \cdot h_e(x_1,x_3,b_1,b_3) \cdot \exp[-S_{ab}(t_a)] \cdot C^{(q)}(t_a,l^2) \\
&+ 2r_K\phi_\pi^A(x_2)\phi_K^P(x_3) \cdot \alpha_s^2(t_b) \cdot h_e(x_3,x_1,b_3,b_1)\exp[-S_{ab}(t_b)] \cdot C^{(q)}(t_b,l'^2)\},
\end{aligned}
\tag{24}
$$

$$
\begin{aligned}
\mathcal{M}_{K^+\pi^-}^{(MP)} = &-16m_{B_s}^6 \frac{C_F^2}{\sqrt{6}} \int_0^1 dx_1 dx_3 \int_0^\infty b_1 db_1 b_2 db_2 b_3 db_3 \phi_{B_s}(x_1) \\
&\cdot \{[(1-x_3)\phi_\pi^A(x_2)[2\phi_K^A(x_3) + r_K(3+x_3)\phi_K^P(x_3) + r_K(1-x_3)\phi_K^T(x_3)] \\
&- r_\pi x_2(1+x_3)(3\phi_\pi^P(x_2)-\phi_\pi^T(x_2))\phi_K^A(x_3)] \\
&\cdot \alpha_s^2(t_a) \cdot h_g(x_i,,b_i) \cdot \exp[-S_{cd}(t_a)] \cdot C_{8g}^{\text{eff}}(t_a) \\
&+ 4r_K\phi_\pi^A(x_2)\phi_K^P(x_3) \cdot \alpha_s^2(t_b)h_g'(x_i,b_i) \cdot \exp[-S_{cd}(t_b)] \cdot C_{8g}^{\text{eff}}(t_b)\},
\end{aligned}
\tag{25}
$$

$$\sqrt{2}\mathcal{M}_{K^0\pi^0}^{(QL)} = \mathcal{M}_{\pi^-K^+}^{(QL)}, \qquad \sqrt{2}\mathcal{M}_{K^0\pi^0}^{(MP)} = \mathcal{M}_{\pi^-K^+}^{(MP)}, \tag{26}$$

$$
\begin{aligned}
\mathcal{M}_{K^+K^-}^{(QL)} = &-8m_{B_s}^4 \frac{C_F^2}{\sqrt{6}} \int_0^1 dx_1 dx_2 dx_3 \int_0^\infty b_1 db_1 b_3 db_3 \phi_{B_s}(x_1) \\
&\times \{[(1+x_3)\phi_K^A(x_2)\phi_K^A(x_3) + r_K(1-2x_3)\phi_K^A(x_2)(\phi_K^P(x_3)+\phi_K^T(x_3)) \\
&+ 2r_k\phi_K^P(x_2)\phi_K^A(x_3)] \cdot \alpha_s^2(t_a) \cdot h_e(x_1,x_3,b_1,b_3) \cdot \exp[-S_{ab}(t_a)] \cdot C^{(q)}(t_a,l^2) \\
&+ 2r_K\phi_k^A(x_2)\phi_K^P(x_3) \cdot \alpha_s^2(t_b) \cdot h_e(x_3,x_1,b_3,b_1) \cdot \exp[-S_{ab}(t_b)] \cdot C^{(q)}(t_b,l'^2)\},
\end{aligned}
\tag{27}
$$

$$
\begin{aligned}
\mathcal{M}_{K^+K^-}^{(MP)} = &-16m_{B_s}^6 \frac{C_F^2}{\sqrt{6}} \int_0^1 dx_1 dx_3 \int_0^\infty b_1 db_1 b_2 db_2 b_3 db_3 \phi_{B_s}(x_1) \\
&\cdot \{[(1-x_3)[2\phi_K^A(x_3) + r_K(3\phi_K^P(x_3)+\phi_K^T(x_3)) + r_K x_3(\phi_K^P(x_3)-\phi_K^T(x_3))]\phi_K^A(x_2) \\
&- r_K x_2(1+x_3)(3\phi_K^P(x_2)-\phi_K^T(x_2))\phi_K^A(x_3)] \\
&\cdot \alpha_s^2(t_a) \cdot h_g(x_i,b_i) \cdot \exp[-S_{cd}(t_a)] \cdot C_{8g}^{\text{eff}}(t_a) \\
&+ 4r_K\phi_K^A(x_2)\phi_K^P(x_3) \cdot \alpha_s^2(t_b) \cdot h_g'(x_i,b_i) \cdot \exp[-S_{cd}(t_b)] \cdot C_{8g}^{\text{eff}}(t_b)\},
\end{aligned}
\tag{28}
$$

$$\mathcal{M}_{\bar{K}^0K^0}^{(QL)} = \mathcal{M}_{K^+K^-}^{(QL)}, \qquad \mathcal{M}_{\bar{K}^0K^0}^{(MP)} = \mathcal{M}_{K^+K^-}^{(MP)}, \tag{29}$$

where the terms proportional to $r_\pi r_K$ or r_K^2 are not shown for the sake of simplicity. The functions h_e, h_g, and h_g', the hard scales t_a and t_b, as well as the Sudakov factors $S_{ab}(t)$ and $S_{cd}(t)$ in Eqs. (24)–(28) will be given in Appendix A.

IV. NUMERICAL RESULTS

In the numerical calculations the following input parameters (here, the masses, decay constants, and QCD scales are in units of GeV) will be used [26,27]:

$$\Lambda_{\overline{\text{MS}}}^{(5)} = 0.225, \qquad f_{B_s} = 0.23 \pm 0.02, \qquad f_K = 0.16, \qquad f_\pi = 0.13,$$

$$M_{B_s} = 5.37, \qquad m_K = 0.494, \qquad m_0^\pi = 1.4, \qquad m_0^K = 1.9,$$

$$\tau_{B_s^0} = 1.497 \text{ ps}, \qquad m_b = 4.8, \qquad M_W = 80.42. \tag{30}$$

For the CKM matrix elements, we also take the same values as being used in Ref. [5], and neglect the small errors on V_{ud}, V_{us}, V_{ts}, and V_{tb}:

$$|V_{ud}| = 0.974, \qquad |V_{us}| = 0.226, \qquad |V_{ub}| = (3.68^{+0.11}_{-0.08}) \times 10^{-3},$$

$$|V_{td}| = (8.20^{+0.59}_{-0.27}) \times 10^{-3}, \qquad |V_{ts}| = 40.96 \times 10^{-3}, \qquad |V_{tb}| = 1.0,$$

$$\alpha = (99^{+4}_{-9.4})°, \qquad \gamma = (59.0^{+9.7}_{-3.7})°, \qquad \arg[-V_{ts}V_{tb}^*] = 1°. \tag{31}$$

A. Branching ratios

For the considered B_s^0 decays, the decay amplitude for a given decay mode with $b \to d, s$ transitions can be generally written as

$$\mathcal{A}(\bar{B}_s^0 \to f)|_{b\to d} = V_{ub}V_{ud}^* T - V_{tb}V_{td}^* P$$
$$= V_{ub}V_{ud}^* T[1 + ze^{i(-\alpha+\delta)}], \tag{32}$$

$$\mathcal{A}(\bar{B}_s^0 \to f)|_{b\to s} = V_{ub}V_{us}^* T' - V_{tb}V_{ts}^* P'$$
$$= V_{ub}V_{us}^* T'[1 + z'e^{i(\gamma+\delta')}], \tag{33}$$

where α and γ are the weak phase (the CKM angles), $\delta = \arg$, $\delta' = \arg[P'/T']$ are the relative strong phases between the tree (T) and penguin (P) diagrams, and the parameter "z" and "z'" are the ratios of penguin to tree contributions with the definition

$$z = \left| \frac{V_{tb}V_{td}^*}{V_{ub}V_{ud}^*} \right| \left| \frac{P}{T} \right|, \qquad z' = \left| \frac{V_{tb}V_{ts}^*}{V_{ub}V_{us}^*} \right| \left| \frac{P'}{T'} \right|. \tag{34}$$

The ratios (z, z') and the strong phases (δ, δ') can be calculated in the pQCD approach. The CP-averaged branching ratio, consequently, can be defined as

$$\text{Br}(\bar{B}_s^0 \to f) = \frac{G_F^2 \tau_{B_s^0}}{32\pi m_B} \frac{1}{2} [|\mathcal{A}(\bar{B}_s^0 \to f)|^2 + |\mathcal{A}(B_s^0 \to \bar{f})|^2], \tag{35}$$

where $\tau_{B_s^0}$ is the lifetime of the B_s^0 meson.

In Table I, we list the pQCD predictions for the averaged branching ratios of the four $\bar{B}_s^0 \to K\pi, KK$ decays. The labels LO and NLO means the pQCD predictions at the leading order only, or with the inclusion of all currently known NLO contributions. The label Set A means the pQCD predictions without the inclusion of the newly known NLO twist-2 and twist-3 contributions to the form factors of $\bar{B}_s^0 \to K$ transitions. For the sake of comparison, we also show the LO pQCD predictions as given in Ref. [5] in the fourth column, and list the NLO theoretical predictions obtained by employing the QCD factorization approach as given in Ref. [8] in the seventh column. The corresponding errors of the previous LO pQCD predictions [5] and the QCDF predictions [8] are the combined total errors. The currently available experimental measurements [26,27] are also shown in the eighth column of Table I.

The main theoretical errors of the NLO pQCD predictions as shown in the sixth column of Table I are induced by the uncertainties of the input parameters. The first dominant error comes from $\omega_b = 0.50 \pm 0.05$ and $f_{B_s} = 0.23 \pm 0.02$ GeV, added in quadrature. The second error arises from the uncertainties of the CKM matrix elements $|V_{ub}|$ and $|V_{cb}|$, as well as the CKM angles α and γ as given

TABLE I. The pQCD predictions for the branching ratios (in units of 10^{-6}) of the four $B_s^0 \to K\pi, KK$ decays. The label "LO" and "NLO" means the leading order and the full next-to-leading order pQCD predictions, while "Set-A" means only NLO twist-2 and twist-3 contributions to form factors are not taken into account. The values listed in the fourth, seventh and eighth column are the LO pQCD predictions [5], the QCDF predictions [8], and currently available data [26,27].

Mode	Class	LO	pQCD [5]	Set A	NLO	QCDF [8]	Data
$\bar{B}_s^0 \to K^+\pi^-$	T	7.30	$7.6^{+3.3}_{-2.5}$	6.4	$5.7^{+2.2+0.5+0.2}_{-1.7-0.6-0.3}$	$10.2^{+6.0}_{-5.2}$	5.4 ± 0.6
$\bar{B}_s^0 \to K^0\pi^0$	C	0.19	$0.16^{+0.12}_{-0.07}$	0.30	$0.28^{+0.10+0.03+0.02}_{-0.06-0.02-0.01}$	$0.49^{+0.62}_{-0.35}$	
$\bar{B}_s^0 \to K^+K^-$	P	13.1	$13.6^{+8.6}_{-5.2}$	20.3	$19.7^{+6.2+2.4+0.2}_{-4.8-2.2-0.2}$	$22.7^{+27.8}_{-13.0}$	24.5 ± 1.8
$\bar{B}_s^0 \to \bar{K}^0K^0$	P	13.3	$15.6^{+9.7}_{-6.0}$	21.2	$20.2^{+6.5+2.4+0.0}_{-4.9-2.2-0.0}$	$24.7^{+29.4}_{-14.0}$	

in Eq. (31). The third error comes from the uncertainties of relevant Gegenbauer moments: $a_1^K = 0.17 \pm 0.05$, $a_2^K = 0.20 \pm 0.06$, and $a_2^\pi = 0.44^{+0.10}_{-0.20}$, added in quadrature again. Here, we assigned roughly a 30% uncertainty for Gegenbauer moments to estimate the resultant errors for the pQCD predictions of the branching ratios.

From the numerical results of the branching ratios, we have the following observations:

(1) The LO pQCD predictions for the branching ratios as given in Ref. [5] are confirmed by our independent calculations. The small differences between the LO pQCD predictions in column three and four are mainly induced by the different choices of the scales $\Lambda_{\text{QCD}}^{(4)}$ and $\Lambda_{\text{QCD}}^{(5)}$: we take $\Lambda_{\text{QCD}}^{(5)} = 0.225$ GeV and $\Lambda_{\text{QCD}}^{(4)} = 0.287$ GeV, instead of the values of $\Lambda_{\text{QCD}}^{(5)} = 0.193$ GeV and $\Lambda_{\text{QCD}}^{(4)} = 0.25$ GeV as being used in Ref. [5].

(2) The NLO contributions can interfere with the LO part constructively or destructively for different decay modes. The inclusion of NLO contributions can lead to a better agreement between the central values of the pQCD predictions and currently available measured values.

(3) The $\bar{B}_s^0 \to K^+\pi^-$ decay is a "tree" dominated decay mode; the NLO contribution leads to a 22% decrease in the central value of the LO pQCD prediction only. For the other three "color-suppressed" and "QCD-penguin" decay modes, however, the NLO contribution leads to ∼50% enhancement to the central values of the LO ones, which in turn play an important role in interpreting the observed large branching ratio $\text{Br}(B_s^0 \to K^+K^-) = (24.5 \pm 1.8) \times 10^{-6}$ [26,27].

(4) When the theoretical errors are taken into account, the NLO pQCD predictions for the branching ratios (in units of 10^{-6}) of the four considered decays are

$$
\begin{aligned}
\text{Br}(\bar{B}_s^0 \to K^+\pi^-) &= 5.7^{+2.3}_{-1.8}, \\
\text{Br}(\bar{B}_s^0 \to K^0\pi^0) &= 0.28^{+0.12}_{-0.07}, \\
\text{Br}(\bar{B}_s^0 \to K^+K^-) &= 19.7^{+6.7}_{-5.3}, \\
\text{Br}(\bar{B}_s^0 \to \bar{K}^0K^0) &= 20.2^{+6.9}_{-5.4},
\end{aligned}
\tag{36}
$$

where the individual errors as shown in the sixth column of Table I have been added in quadrature. One can see that the theoretical errors of the NLO pQCD predictions are a little smaller than those of the LO ones, but still similar with them. Such a small change of the size of the theoretical error is consistent with the general expectation. Of course, we know that although the agreement between the central values of the pQCD predictions and the data are improved effectively due to the inclusion of NLO contributions; the theoretical errors of the pQCD predictions are roughly 35% of the

central values, and still large when compared with the less than 10% uncertainty of the measured values.

B. *CP*-violating asymmetries

Now we turn to the evaluations of the *CP*-violating asymmetries of the considered four B_s^0 decays in the pQCD approach. For $B_s^0 \to K^\mp\pi^\pm$ decays, the definition for its direct *CP*-violating asymmetry is very simple [1]. For neutral B_s^0 decays into a *CP* eigenstate $\bar{f} = \eta_{CP}f$ with $\eta_{CP} = \pm 1$ for the *CP*-even and *CP*-odd final states, the time-dependent *CP* asymmetry can be defined as [2,28]

$$
\begin{aligned}
\mathcal{A}(t) &= \frac{\Gamma_{\bar{B}_s^0 \to f}(t) - \Gamma_{B_s^0 \to f}(t)}{\Gamma_{\bar{B}_s^0 \to f}(t) + \Gamma_{B_s^0 \to f}(t)} \\
&= \frac{\mathcal{A}_f \cos(\Delta m_s t) + \mathcal{S}_f \sin(\Delta m_s t)}{\cosh\left(\frac{\Delta\Gamma_s}{2}t\right) + \mathcal{H}_f \sinh\left(\frac{\Delta\Gamma_s}{2}t\right)},
\end{aligned}
\tag{37}
$$

where Δm_s and $\Delta\Gamma_s$ are the mass and width differences of the $B_s^0 - \bar{B}_s^0$ system mass eigenstates. The direct *CP*-violating asymmetry $\mathcal{A}_f$ and the mixing-induced *CP*-violating asymmetry $\mathcal{S}_f$ and $\mathcal{H}_f$ are defined as in Refs. [2,28]:

$$
\mathcal{A}_f = \frac{|\lambda_f|^2 - 1}{1 + |\lambda_f|^2}, \qquad \mathcal{S}_f = \frac{2\,\text{Im}\lambda_f}{1 + |\lambda_f|^2}, \qquad \mathcal{H}_f = \frac{2\,\text{Re}\lambda_f}{1 + |\lambda_f|^2},
\tag{38}
$$

where the three factors satisfy the normalization relation: $|\mathcal{A}_f|^2 + |\mathcal{S}_f|^2 + |\mathcal{H}_f|^2 = 1$, and the *CP*-violating parameter λ_f is defined as

$$
\lambda_f = \frac{q}{p}\frac{\bar{A}_f}{A_f} = \eta_f e^{2i\epsilon}\frac{A(\bar{B}_s \to f)}{A(B_s \to f)},
\tag{39}
$$

where $\epsilon = \arg[-V_{ts}V_{tb}^*]$ is very small in size and can be neglected safely. It is worth mentioning that the parameters $\mathcal{A}_f$ and $\mathcal{H}_f$ defined in Eqs. (37) and (38) have an opposite sign as the parameter $\mathcal{C}_f$ and $\mathcal{A}_f^{\Delta\Gamma}$ as defined in Ref. [2], i.e., $\mathcal{A}_f = -\mathcal{C}_f$ and $\mathcal{H}_f = -\mathcal{A}_f^{\Delta\Gamma}$.

In Tables II and III, we list the pQCD predictions (in units of 10^{-2}) for the direct *CP*-violating asymmetry $\mathcal{A}_f$ and the mixing-induced *CP*-violating asymmetry $\mathcal{S}_f$ and $\mathcal{H}_f$ of the considered B_s^0 decays, respectively. As a comparison, the LO pQCD predictions as given in Ref. [5], the QCDF predictions as given in Ref. [8], and the measured values [1,2] are listed in Table II and Table III. The errors of our NLO pQCD predictions for *CP*-violating asymmetries are defined in the same way as those for the branching ratios.

From the pQCD predictions and currently available data for the *CP*-violating asymmetries of the considered $\bar{B}_s^0$ decays, we find that (a) the LO pQCD predictions obtained in this paper agree well with those as given in Ref. [5]; (b)

TABLE II. The same format as in Table I, but for the pQCD predictions (in unit of 10^{-2}) for the direct CP asymmetries $\mathcal{A}_f$. The previous LO pQCD predictions [5], the QCDF predictions [8], and the measured values [1,2] are also listed.

Mode	Class	LO	pQCD [5]	Set A	NLO	QCDF [8]	Data
$\bar{B}_s^0 \to K^+\pi^-$	T	27.6	$24.1^{+5.6}_{-4.8}$	36.2	$38.7^{+5.0+2.1+2.2}_{-5.0-1.8-1.8}$	$-6.7^{+15.6}_{-15.3}$	27 ± 4 [1]
$\bar{B}_s^0 \to K_S^0\pi^0$	C	62.9	$59.4^{+7.9}_{-12.5}$	84.8	$83.0^{+5.8+3.4+2.3}_{-5.6-2.6-2.7}$	42^{+47}_{-56}	
$\bar{B}_s^0 \to K^+K^-$	P	-13.7	$-23.3^{+5.0}_{-4.6}$	-17.1	$-16.4^{+0.3+0.6+0.6}_{-0.1-0.4-0.6}$	$4.0^{+10.6}_{-11.6}$	-14 ± 12[2]
$\bar{B}_s^0 \to \bar{K}^0 K^0$	P	0	0	-0.7	-0.7 ± 0.1	0.3 ± 0.1	

TABLE III. The same format as in Table I, but for the pQCD predictions (in units of 10^{-2}) for the mixing-induced CP asymmetries $\mathcal{S}_f$ and $\mathcal{H}_f$ (the second row). The previous LO pQCD predictions [5], the QCDF predictions [9], and the measured values [1,2] are also listed.

Mode	Class	LO	pQCD [5]	Set A	NLO	QCDF [9]	Data [2]
$\bar{B}_s^0 \to K_S^0\pi^0$	C	-56.2	-61^{+24}_{-20}	-50.0	$-52.9^{+8.0+4.2+4.7}_{-8.2-4.3-4.4}$	45	
		-53.7	-52^{+23}_{-17}	-17.8	$-17.4^{+0.9+2.0+4.8}_{-0.1-1.0-4.1}$	$-$	
$\bar{B}_s^0 \to K^+K^-$	P	37.1	28^{+5}_{-5}	22.0	$20.6^{+1.9+1.4+0.8}_{-1.8-1.3-0.7}$	27	30 ± 13
		92.0	93^{+3}_{-3}	96.0	$96.5^{+0.3+0.1+0.1}_{-0.4-0.2-0.2}$	$-$	
$\bar{B}_s^0 \to \bar{K}^0 K^0$	P	$-$	4	-0.2	-0.2	-3.5	
		100	~100	~100	~100	$-$	

for the CP-violating asymmetries of the considered $\bar{B}_s^0$ decays, the effects of the NLO contributions are small or moderate in size; and (c) for $\bar{B}_s^0 \to K^\pm\pi^\mp$ and $\bar{B}_s^0 \to K^+K^-$ decays, the pQCD predictions for both $\mathcal{A}_f$ and $\mathcal{S}_f$ agree well with those measured values in both the sign and the magnitude when still large theoretical and experimental errors are taken into account.

V. SUMMARY

In this paper, we calculated the branching ratios and CP-violating asymmetries of the four $\bar{B}_s^0 \to K\pi, KK$ decays, with the inclusion of all known NLO contributions, especially the NLO twist-2 and twist-3 contributions to the form factors to the $B_s \to K$ transition. From our calculations and phenomenological analysis, we found the following results:

(1) For the considered four decays, the NLO contribution can interfere with the LO part constructively or destructively for different decay modes. The currently available data can be interpreted by the inclusion of the NLO contribution.

(2) For $\mathrm{Br}(\bar{B}_s^0 \to K^+\pi^-)$, the NLO contribution leads to a 22% decrease to the central value of the LO pQCD prediction. For the other three decay modes, however, the NLO contributions can provide $\sim50\%$ enhancements to the central values of the LO ones and therefore play an important role in interpreting the observed large branching ratio $\mathrm{Br}(\bar{B}_s^0 \to K^+K^-) = (24.5 \pm 1.8) \times 10^{-6}$.

(3) For the CP-violating asymmetries, the effects of the NLO contributions are small or moderate in size. For

$\bar{B}_s^0 \to K^+\pi^-$ and $\bar{B}_s^0 \to K^+K^-$ decays, the pQCD predictions for the direct and mixing-induced CP-violating asymmetries agree well with the measured values in both the sign and the magnitude.

(4) For the branching ratios of the four considered decays, the agreement between the central values of the pQCD predictions and the data are improved effectively due to the inclusion of the NLO contributions, but the theoretical errors of the pQCD predictions are still relatively large, say about 35% of the central values, when compared with $\sim10\%$ uncertainty of the measured values. The main sources of the theoretical errors come from the uncertainties of the input parameters, such as ω_b, f_{B_s}, a_2^π, etc. More works should be done to improve the accuracy of the theoretical predictions.

APPENDIX: RELATED HARD FUNCTIONS AND SUDAKOV FACTOR

We list here the hard function h_i and the Sudakov factors $S_{ab}(t)$ and $S_{cd}(t)$ appeared in the expressions of the decay amplitudes in Eqs. (24)–(28). The hard functions $h_i(x_j, b_j)$ are obtained by making the Fourier transformations of the hard kernel $H^{(0)}$:

$$h_e(x_1, x_3, b_1, b_3) = [\theta(b_1 - b_3)I_0(\sqrt{x_3}m_{B_s}b_3)K_0(\sqrt{x_3}m_{B_s}b_1) + \theta(b_3 - b_1)I_0(\sqrt{x_3}m_{B_s}b_1) \cdot K_0(\sqrt{x_3}m_{B_s}b_3)]$$
$$\cdot K_0(\sqrt{x_1 x_3}m_{B_s}b_1)S_t(x_3), \tag{A1}$$

$$h_g(x_i, b_i) = -\frac{i\pi}{2}S_t(x_3)[J_0(\sqrt{x_2\bar{x}_3}m_{B_s}b_2) + iN_0(\sqrt{x_2\bar{x}_3}m_{B_s}b_2)] \cdot K_0(\sqrt{x_1 x_3}M_{B_s}b_1)$$
$$\cdot \int_0^{\pi/2} d\theta \tan\theta \cdot J_0(\sqrt{x_3}m_{B_s}b_1\tan\theta)J_0(\sqrt{x_3}m_{B_s}b_2\tan\theta) \cdot J_0(\sqrt{x_3}m_{B_s}b_3\tan\theta), \tag{A2}$$

$$h'_g(x_i, b_i) = -S_t(x_1)K_0(\sqrt{x_1 x_3}m_{B_s}b_3) \cdot \int_0^{\pi/2} d\theta \tan\theta \cdot J_0(\sqrt{x_1}m_{B_s}b_1\tan\theta) \cdot J_0(\sqrt{x_1}m_{B_s}b_2\tan\theta)J_0(\sqrt{x_1}m_{B_s}b_3\tan\theta)$$
$$\times \begin{cases} \frac{i\pi}{2}[J_0(\sqrt{x_2 - x_1}m_{B_s}b_2) + iN_0(\sqrt{x_2 - x_1}m_{B_s}b_2)], & x_1 < x_2, \\ K_0(\sqrt{x_1 - x_2}m_{B_s}b_2), & x_1 > x_2, \end{cases} \tag{A3}$$

with K_0, I_0, and J_0 as the Bessel functions [29]. And the threshold resummation form factor $S_t(x_i)$ can be found in Ref. [25].

The Sudakov factors that appeared in Eqs. (24)–(28) are defined as

$$S_{ab}(t) = s\left(x_1\frac{m_{B_s}}{\sqrt{2}}, b_1\right) + s\left(x_3\frac{m_{B_s}}{\sqrt{2}}, b_3\right) + s\left(\bar{x}_3\frac{m_{B_s}}{\sqrt{2}}, b_3\right) + \frac{5}{3}\int_{1/b_1}^t d\mu\frac{\gamma_q(\alpha_s(\mu))}{\mu} + 2\int_{1/b_3}^t d\mu\frac{\gamma_q(\alpha_s(\mu))}{\mu}, \tag{A4}$$

$$S_{cd}(t) = s\left(x_1\frac{m_{B_s}}{\sqrt{2}}, b_1\right) + s\left(x_2\frac{m_{B_s}}{\sqrt{2}}, b_2\right) + s\left(\bar{x}_2\frac{m_{B_s}}{\sqrt{2}}, b_2\right) + s\left(x_3\frac{m_{B_s}}{\sqrt{2}}, b_1\right) + s\left(\bar{x}_3\frac{m_{B_s}}{\sqrt{2}}, b_1\right)$$
$$+ \frac{11}{3}\int_{1/b_1}^t d\mu\frac{\gamma_q(\alpha_s(\mu))}{\mu} + 2\int_{1/b_2}^t d\mu\frac{\gamma_q(\alpha_s(\mu))}{\mu}, \tag{A5}$$

where $\bar{x}_i = 1 - x_i$; the function $s(Q, b)$ can be found in Refs. [30,31]. The hard scales t_a and t_b that appeared in Eqs. (24)–(28) take the form of

$$t_a = \max\{\sqrt{x_1 x_3}m_{B_s}, \sqrt{x_3}m_{B_s}, \sqrt{x_2(1 - x_3)}m_{B_s}, 1/b_1, 1/b_3\},$$
$$t_b = \max\{\sqrt{x_1 x_3}m_{B_s}, \sqrt{x_1}m_{B_s}, \sqrt{|x_1 - x_2|}m_{B_s}, 1/b_1, 1/b_3\}, \tag{A6}$$

where the energy scale $\sqrt{x_2(1 - x_3)}m_{B_s}$ and $\sqrt{|x_1 - x_2|}m_{B_s}$ come from the invariant mass of the gluon $l^2 = x_2(1 - x_3)m_{B_s}^2$ and $l'^2 = (x_1 - x_2)m_{B_s}^2$. They are chosen as the maximum energy scale appearing in each diagram to kill the large logarithmic radiative corrections.

[1] R. Aaij *et al.* (LHCb Collaboration), Phys. Rev. Lett. **108**, 201601 (2012); **110**, 221601 (2013).

[2] R. Aaij *et al.* (LHCb collaboration), J. High Energy Phys. 10 (2013) 183; R. Aaij *et al.* (LHCb collaboration), Phys. Lett. B **716**, 393 (2012).

[3] Y. Li, C. D. Lü, Z. J. Xiao, and X. Q. Yu, Phys. Rev. D **70**, 034009 (2004); X. Q. Yu, Y. Li, and C. D. Lü, Phys. Rev. D **71**, 074026 (2005); **73**, 017501 (2006); J. Zhu, Y. L. Shen, and C. D. Lü, J. Phys. G **32**, 101 (2006).

[4] Z. J. Xiao, X. Liu, and H. S. Wang, Phys. Rev. D **75**, 034017 (2007).

[5] A. Ali, G. Kramer, Y. Li, C. D. Lü, Y. L. Shen, W. Wang, and Y. M. Wang, Phys. Rev. D **76**, 074018 (2007).

[6] J. Liu, R. Zhou, and Z. J. Xiao, arXiv:0812.2312.

[7] Y. H. Chen, H. Y. Cheng, and B. Tseng, Phys. Rev. D **59**, 074003 (1999).

[8] M. Beneke and M. Neubert, Nucl. Phys. **B675**, 333 (2003).

[9] J. F. Sun, G. H. Zhu, and D. S. Du, Phys. Rev. D **68**, 054003 (2003).

[10] H. Y. Cheng and C. K. Chua, Phys. Rev. D **80**, 114026 (2009).

[11] Z. J. Xiao, Z. Q. Zhang, X. Liu, and L. B. Guo, Phys. Rev. D **78**, 114001 (2008).

[12] Y. Y. Fan, W. F. Wang, S. Cheng, and Z. J. Xiao, Phys. Rev. D **87**, 094003 (2013).

[13] W. Bai, M. Liu, Y. Y. Fan, W. F. Wang, S. Cheng, and Z. J. Xiao, Chinese Phys. C **38**, 033101 (2014).

[14] H. N. Li, S. Mishima, A. I. Sanda, Phys. Rev. D **72**, 114005 (2005).

[15] H. N. Li, Y. L. Shen, and Y. M. Wang, Phys. Rev. D **85**, 074004 (2012).

[16] S. Cheng, Y. Y. Fan, X. Yu, C. D. Lü, and Z. J. Xiao, arXiv:1402.5501v2.

[17] J. Botts and G. Sterman, Nucl. Phys. **B325**, 62 (1989); H. N. Li and G. Sterman, Nucl. Phys. **B381**, 129 (1992); T. Huang and Q. X. Shen, Z. Phys. C **50**, 139 (1991); F. G. Cao, T. Huang, and C. W. Luo, Phys. Rev. D **52**, 5358 (1995).

[18] H. N. Li, Prog. Part. Nucl. Phys. **51**, 85 (2003) and references therein.

[19] G. Buchalla, A. J. Buras, and M. E. Lautenbacher, Rev. Mod. Phys. **68**, 1125 (1996).

[20] V. M. Braun and I. E. Filyanov, Z. Phys. C **48**, 239 (1990); P. Ball, V. M. Braun, Y. Koike, and K. Tanaka, Nucl. Phys. **B529**, 323 (1998); P. Ball, J. High Energy Phys. 01 (1999) 010.

[21] V. M. Braun and A. Lenz, Phys. Rev. D **70**, 074020 (2004); P. Ball and A. Talbot, J. High Energy Phys. 06 (2005) 063; P. Ball and R. Zwicky, Phys. Lett. B **633**, 289 (2006); A. Khodjamirian, Th. Mannel, and M. Melcher, Phys. Rev. D **70**, 094002 (2004).

[22] X. G. Wu and T. Huang, arXiv:1312.1355.

[23] S. Mishima and A. I. Sanda, Prog. Theor. Phys. **110**, 549 (2003).

[24] M. Beneke, G. Buchalla, M. Neubert, and C. T. Sachrajda, Phys. Rev. Lett. **83**, 1914 (1999); M. Beneke, G. Buchalla, M. Neubert, and C. T. Sachrajda, Nucl. Phys. **B591**, 313 (2000).

[25] T. Kurimoto, H. N. Li, and A. I. Sanda, Phys. Rev. D **65**, 014007 (2001); C. D. Lu and M. Z. Yang, Eur. Phys. J. C **28**, 515 (2003).

[26] Y. Amhis *et al.* (Heavy Flavor Averaging Group), arXiv:1207.1158v2.

[27] J. Beringer *et al.* (Particle Data Group), Phys. Rev. D **86**, 010001 (2012).

[28] I. Dunietz, Phys. Rev. D **52**, 3048 (1995).

[29] I. S. Gradshteyn and I. M. Ryzhik, *Table of Integrals, Series, and Products* (Academic Press, New York, 1980).

[30] H. N. Li and K. Ukai, Phys. Lett. B **555**, 197 (2003).

[31] H. N. Li and B. Melic, Eur. Phys. J. C **11**, 695 (1999).